The 21st Annual IEEE International Symposium on Personal, Indoor and Mobile Radio Communications (PIMRC'10)

Carrier Frequency Synchronization in the Downlink of 3GPP LTE

Qi Wang, Christian Mehlführer, and Markus Rupp

Institute of Communications and Radio-Frequency Engineering
Vienna University of Technology
Gusshausstrasse 25/389, A-1040 Vienna, Austria
Email: {qwang,chmehl,mrupp}@nt.tuwien.ac.at
Web: http://www.nt.tuwien.ac.at/rapid-prototyping

***Abstract*—In this paper, we investigate carrier frequency synchronization in the downlink of 3GPP Long Term Evolution (LTE). A complete carrier frequency offset estimation and compensation scheme based on standardized synchronization signals and reference symbols is presented. The estimation performance in terms of mean square error is derived analytically and compared to simulation results. The impact of estimation error on the system performance is shown in terms of uncoded bit error ratio and physical layer coded throughput. Compared to perfect synchronization, the presented maximum likelihood estimator shows hardly any performance loss, even when the most sophisticated MIMO schemes of LTE are employed.**

I. Introduction

Long Term Evolution (LTE) [1] has been standardized as the successor of the Universal Mobile Telecommunication System (UMTS). The downlink transmission utilizes Orthogonal Frequency Division Multiple Access (OFDMA) as the physical layer technique which enables high data rate transmission in frequency selective fading scenarios. However, one of the drawbacks of OFDMA is its vulnerability to Carrier Frequency Offset (CFO). Given a carrier frequency of 2.5 GHz, a typical frequency drift of 10ppm (10×10^{-6}) of the local oscillator results in an offset of 25 kHz. In LTE, which employs a fixed subcarrier spacing of 15 kHz, such an offset corresponds to 1.67 subcarrier spacings.

Synchronization for general OFDM systems has been investigated for example in [2–8]. The basic idea in these publications is to split the CFO into a Fractional Frequency Offset (FFO), an Integer Frequency Offset (IFO), and a Residual Frequency Offset (RFO), which can be estimated individually. In [2–4], a Cyclic Prefix (CP) based FFO estimator has been presented and the Cramer-Rao lower bound of this estimator has been derived in [8]. In order to expand the estimation range, an IFO estimator based on the maximum likelihood principle has been derived in [5]. The impact of RFO as well as RFO compensation schemes were investigated in [4, 6, 7]. Specifically for LTE, a synchronization concept was presented in [9]. However, the performance was only evaluated in terms of *simulated* Mean Squared Error (MSE).

In this work, we present an entire chain of carrier frequency offset estimation blocks based on the standardized synchronization signals and reference symbols of LTE. Furthermore, we derive *analytic* expressions for the MSE of the RFO and the FFO estimators. The mathematical analysis is complemented by simulations that are carried out using a standard compliant MATLAB-based downlink physical layer simulator for LTE [10]. In addition to the frequency offset MSE, also the system performance after compensation is evaluated in terms of uncoded bit error ratio and physical layer coded throughput. All algorithm implementations will be made publicly available in a future release of our LTE physical layer simulator [10].

The paper is organized as follows. In Section II, the standardized synchronization and reference signals of LTE are described. Section III explains our system model and the impact of CFO on an OFDM system. Our carrier frequency offset estimation scheme and its analytical MSE are presented in Section IV. Section V shows the physical layer simulation results. Finally we draw our conclusions in Section VI.

II. Synchronization and Reference Signals in LTE

As specified in [11], radio frames in an LTE downlink transmission have a duration of $T_{\text{frame}} = 10\,\text{ms}$. Each frame consists of 10 subframes of equal length. Each subframe contains two consecutive slots of time duration $T_{\text{slot}} = 0.5\,\text{ms}$. The smallest scheduling unit is called one resource block which is a time-frequency grid of 12 subcarriers over $N_{\text{s}} = 7$ OFDM symbols for the normal CP length and $N_{\text{s}} = 6$ for the extended CP length. In the LTE downlink two kinds of signals can be utilized for synchronization at the receiver. Firstly, the dedicated synchronization signals, and secondly the cell-specific reference symbols. Both are briefly explained below.

A. Synchronization Signals

The LTE standard defines two synchronization signals, namely the primary (PSCH) and the secondary (SSCH). In FDD mode, these signals are located on the 62 subcarriers symmetrically arranged around the DC-carrier in the first slot in the sixth and seventh OFDM symbols of the first and the sixth subframes, as shown in Fig. 1.

B. Cell-specific Reference Symbols

Cell-specific reference signals utilize 4-QAM modulated symbol alphabets and are mapped to the resource elements

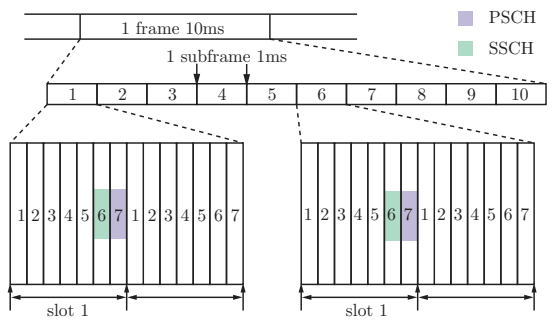

Fig. 1. Synchronization signals in LTE FDD downlink.

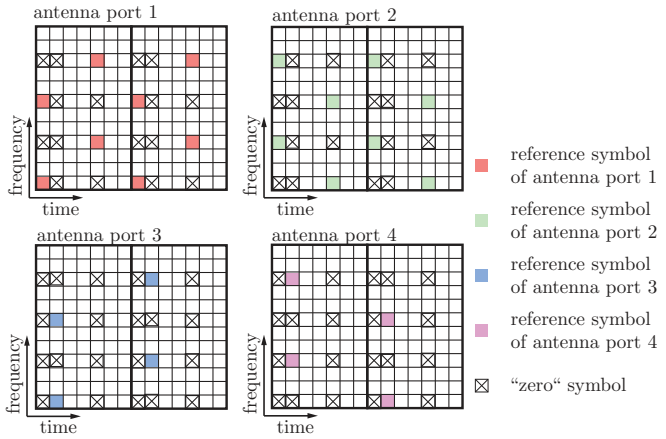

Fig. 2. Cell-specific reference signals in LTE FDD downlink.

in the frequency domain as shown in Fig. 2. Whenever there is one antenna port transmitting a reference symbol on one resource element, all the other antenna ports transmit a "zero" symbol at this position. Thus, interference of the reference symbols transmitted from different antennas is avoided and channel estimation is simplified.

III. Carrier Frequency Offset in OFDM

In this section, we define an OFDM system model and show what impact a carrier frequency offset has on the OFDM signal. The transmitted time-domain OFDM signal is denoted by $x_{l,n}^{(m)}$, the channel impulse response by $h_{l,n}^{(m)}$, the additive Gaussian noise by $v_{l,n}^{(m)}$, and the received time-domain signal by $r_{l,n}^{(m)}$. Here, l is the OFDM symbol index within one subframe, $n \in [1, N + N_\mathrm{g}]$ the time index within one OFDM symbol and m the receive antenna index. N denotes the FFT size and N_g the CP length.

Using the above definitions, the transmission with CFO is described in the time-domain as

$$r_{l,n}^{(m)} = \left\{ x_{l,n}^{(m)} * h_{l,n}^{(m)} + v_{l,n}^{(m)} \right\} \cdot e^{j2\pi\varepsilon_\mathrm{CFO}(n+l(N+N_\mathrm{g}))/N}, \quad (1)$$

where ε_CFO is the frequency mismatch between transmitter and receiver carrier frequency normalized to the subcarrier spacing.

Correspondingly, we define in the frequency-domain $X_{l,k}^{(m)}$ as the transmitted symbol, $H_{l,k}^{(m)}$ as the channel frequency response, $V_{l,k}^{(m)}$ as the additive Gaussian noise, and $R_{l,k}^{(m)}$ as the received symbol on the k-th subcarrier of the l-th OFDM symbol at the m-th receive antenna. When the discrete Fourier transform is applied to the received signal $r_{l,n}^{(m)}$ in Eq. (1), we obtain according to [2]

$$R_{l,k}^{(m)} = \gamma \cdot X_{l,k'}^{(m)} H_{l,k'}^{(m)} + I_{l,k'}^{(m)} + \tilde{V}_{l,k}^{(m)}, \quad (2)$$

with

$$\gamma = \frac{\sin(\pi\varepsilon')}{N\sin(\pi\varepsilon'/N)} \cdot e^{j\pi\varepsilon'(N-1)/N} \cdot e^{j2\pi\varepsilon_\mathrm{CFO} l(N+N_\mathrm{g})/N}, \quad (3)$$

$$I_{l,k'}^{(m)} = \sum_{p \neq k'} X_{l,p}^{(m)} H_{l,p}^{(m)} \cdot \frac{\sin(\pi(p+\varepsilon_\mathrm{CFO}-k))}{N\sin(\pi(p+\varepsilon_\mathrm{CFO}-k)/N)} \cdot e^{j\pi(p+\varepsilon_\mathrm{CFO}-k)(N-1)/N} \cdot e^{j2\pi\varepsilon_\mathrm{CFO} l(N+N_\mathrm{g})/N}. \quad (4)$$

where the relations $k' = k - \varepsilon_\mathrm{IFO}$ and $\varepsilon' = \varepsilon_\mathrm{CFO} - \varepsilon_\mathrm{IFO} = \varepsilon_\mathrm{FFO} + \varepsilon_\mathrm{RFO}$ are used. The last relation is obtained because the total CFO can be split into the FFO, IFO, and the RFO: $\varepsilon_\mathrm{CFO} = \varepsilon_\mathrm{FFO} + \varepsilon_\mathrm{IFO} + \varepsilon_\mathrm{RFO}$. The factor γ is the degradation on the desired subcarrier caused by the CFO. $I_{l,k'}^{(m)}$ contains the inter-carrier interference from the neighboring subcarriers. The index k' implies that data symbols transmitted on subcarrier $k - \varepsilon_\mathrm{IFO}$ are received on subcarrier k.

IV. Carrier Frequency Offset Estimation Scheme

In this section, we develop a three-stage CFO compensation scheme for UMTS LTE. We assume the channel to be slow fading, that is, the variation of the channel impulse response within one subframe of duration 1 ms is negligible.

A. FFO Estimation

As shown in Eq. (3) and (4), FFO is the major source of inter-carrier interference destroying the orthogonality between subcarriers. Therefore, it has to be compensated before the FFT operation in the OFDM receiver.

In [3], a Maximum Likelihood (ML) estimator for the FFO has been derived. In the context of slow fading, this method can be extended to subframe base as below:

$$\hat{\varepsilon}_\mathrm{FFO} = -\frac{1}{2\pi} \arg\left\{ \sum_{m=1}^{N_\mathrm{R}} \sum_{l=1}^{N_\mathrm{f}} \sum_{n=1}^{N_\mathrm{g}} r_{l,n}^{(m)} r_{l,n+N}^{(m)*} \right\}. \quad (5)$$

In this equation, N_R denotes the number of receive antennas, N_f the number of OFDM symbols in one subframe, and N_g the CP length. The estimation range (normalized to the subcarrier spacing) of this stage is $(-0.5, 0.5)$ and is determined by the $\arg\{\cdot\}$ operation. In an AWGN channel where sufficiently large SNR is assumed, the MSE of this FFO estimator can be derived as

$$\mathrm{MSE}_{\varepsilon_\mathrm{FFO}} = \frac{2\sigma_v^2\sigma_r^2 + \sigma_v^4}{8\pi^2 N_\mathrm{R} N_\mathrm{g} N_\mathrm{f} \sigma_r^4} = \frac{2\gamma_t + 1}{8\pi^2 N_\mathrm{R} N_\mathrm{g} N_\mathrm{f} \gamma_t^2} \approx \approx \frac{1}{4\pi^2 N_\mathrm{R} N_\mathrm{g} N_\mathrm{f} \gamma_t}, \quad (6)$$

where $\gamma_t = \sigma_r^2/\sigma_v^2 \gg 1$ is the signal-to-noise ratio of the received signal in time domain. A detailed derivation of Eq. (6) is provided in Appendix I.

It is obvious that the estimation error can be reduced by using more receive antennas, by extending the CP length, or by taking more OFDM symbols into account.

B. IFO Estimation

After the FFO estimation stage, we assume the fractional part of the CFO has been mostly corrected. It can be seen from Eq. (2) and Eq. (3) that the integer part of the CFO has two effects on the received signal. The first is the FFT index shift, that is, the symbol transmitted on subcarrier $k - \varepsilon_{\text{IFO}}$ is received on subcarrier k. The second effect is a phase rotation proportional to the OFDM index l.

These two effects can be compensated once the IFO is estimated, for example by the ML estimator proposed in [5]. The symbols used for estimation can be either pre-defined pilots or PSK modulated data symbols. In the context of LTE, we choose to only apply it to the standardized synchronization signals, leading to the following IFO estimator:

$$\hat{\varepsilon}_{\text{IFO}} = \arg\max_i \left\{ \Re\left[e^{\frac{j2\pi i N_{\text{g}}}{N}} \cdot \right.\right. \tag{7}$$
$$\left.\left. \cdot \sum_{m=1}^{N_{\text{R}}} \sum_{k \in K_{\text{SCH}}} \left(R^{(m)*}_{\text{SSCH},k+i} R^{(m)}_{\text{PSCH},k+i} \right) \left(X^{(m)*}_{\text{SSCH},k} X^{(m)}_{\text{PSCH},k} \right)^* \right] \right\},$$

where $\Re\{\cdot\}$ returns the real part of the argument and $i \in (-31, 31)$ corresponds to the set of potential integer offsets that can be estimated. This set is determined by the definition of the synchronization signals in LTE. The set K_{SCH} represents the subcarrier indices that contain the synchronization signals. Note that due to the fact that in LTE the synchronization signals only exist in every fifth subframe, the estimation of ε_{IFO} can only be carried out in these subframes.

C. RFO Estimation

The magnitude of the RFO depends on the estimation error of the FFO. Although its impact on the current OFDM symbol may not be visible, the estimation error leads to an increasing phase shift for subsequent OFDM symbols, see Eq. (1). Therefore, it is necessary to improve the estimation by using the cell-specific reference signals to correct the RFO after the FFT.

Given Eq. (2) and Eq. (3), we assume $\hat{\varepsilon}_{\text{FFO}}$ and $\hat{\varepsilon}_{\text{IFO}}$ have been corrected to the extent that the interference is small enough to be neglected. When two symbols on subcarrier k in OFDM symbols l and $l + L$ are observed, there is

$$W^{(m)}_{l,k} = R^{(m)}_{l,k} R^{(m)*}_{l+L,k} \cdot \left(X^{(m)}_{l,k} X^{(m)*}_{l+L,k} \right)^* = \tag{8}$$
$$= e^{-j2\pi\varepsilon_{\text{RFO}} L(N+N_{\text{g}})/N} \cdot |X^{(m)}_{l,k}|^2 |X^{(m)}_{l+L,k}|^2 |H^{(m)}_{l,k}|^2 + \tilde{V}^{(m)}_{l,k}.$$

The RFO ε_{RFO} is only contained in the argument of the signal term. This holds under the assumption that the channel does not change during L OFDM symbols. When applied to the cell-specific reference signals in LTE, $L = N_{\text{s}}$ is the number of OFDM symbols in one slot. The corresponding RFO estimator can be expressed as

$$\hat{\varepsilon}_{\text{RFO}} = -\frac{1}{2\pi} \frac{N}{N_{\text{s}}(N + N_{\text{g}})} \cdot \tag{9}$$
$$\cdot \arg\left\{ \sum_m \sum_{(k,l) \in K_{\text{P}}} R^{(m)}_{l,k} R^{(m)*}_{l+N_{\text{s}},k} \cdot \left(X^{(m)}_{l,k} X^{(m)*}_{l+N_{\text{s}},k} \right)^* \right\}.$$

The estimation is performed on subframe basis with the set K_{P} corresponding to the joint set of subcarrier indices and OFDM symbol numbers on which the reference symbols are located.

Similar to the FFO estimation, the estimation range for ε_{RFO} is $(-N/(2N_{\text{s}}(N + N_{\text{g}})), N/(2N_{\text{s}}(N + N_{\text{g}})))$. Specifically, for the 5 MHz mode with normal CP length, $\hat{\varepsilon}_{\text{RFO}} \in (-0.067, 0.067)$. The derivation of the theoretical MSE is similar to that of the FFO estimator and results in

$$\text{MSE}_{\varepsilon_{\text{RFO}}} \approx \frac{N^2}{4\pi^2 N_{\text{s}}^2 (N + N_{\text{g}})^2 N_{\text{R}} K \gamma_f}, \tag{10}$$

where $\gamma_f = \sigma_s^2/\sigma_v^2$ is the post-FFT signal-to-noise ratio. In LTE, the factor K is the total number of reference symbols in one slot. Specifically for the 5 MHz mode we have $K = 100$ when one transmit antenna port is used and $K = 200$ when two transmit antenna ports are used. Since the RFO estimator relies on pairs of reference symbols located on the same subcarrier, the reference signals of antenna ports three and four have no contribution.

TABLE I
SIMULATOR PARAMETERS FOR SIMULATIONS WITH CFO

Parameter	Value
Bandwidth	5 MHz
Transmission setting	1×1, 2×2, 4×2
Number of users	1
CQI	9
Symbol alphabet	16QAM
Coding rate	$616/1024 = 0.602$
Transmission mode	Open loop spatial multiplexing
Maximum HARQ retransmission	0
Channel model	AWGN[1]/ITU PedB [12]
OFDM symbol timing	Perfect
Channel estimation	Perfect
Receiver type	Soft sphere decoder
Number of subframes	1000
Introduced CFO	3.1415 subcarrier spacings

V. SIMULATION RESULTS

In this section, we present simulation results and evaluate the performance of the CFO compensation scheme. Simulations are carried out using a standard compliant LTE link level simulator that was developed at the Vienna University of Technology [13]. According to Eq. (6),(10), the frequency offset estimation error does not depend on the magnitude of the CFO. Therefore, we introduced a constant CFO and evaluate the system performance comparing to a perfectly synchronized

[1]The channel matrix of the 4×2 AWGN channel is defined as $[1\ 1\ 1\ 1; 1\ -1\ -1\ 1]$.

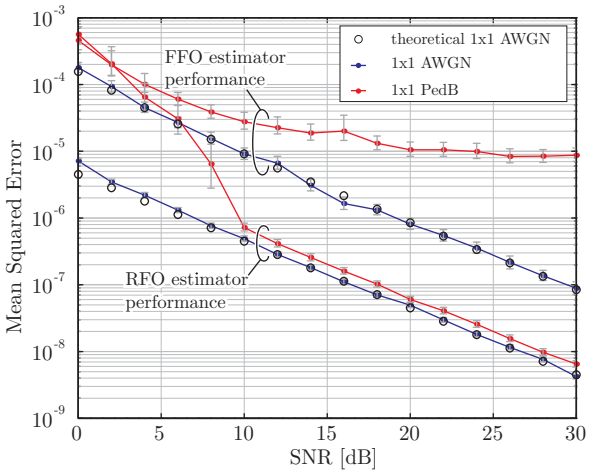

Fig. 3. Calculated and simulated Mean Squared Error for FFO and RFO in 1×1 transmission.

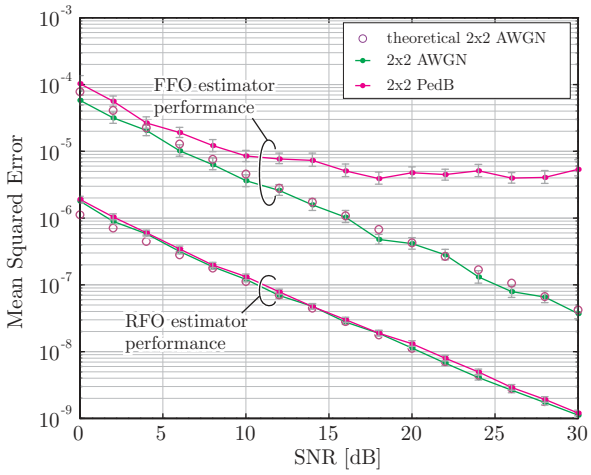

Fig. 4. Calculated and simulated Mean Squared Error for FFO and RFO in 4×2 transmission.

transmission. According to [14], sampling frequencies on both ends are assumed to be perfectly synchronized. The other simulation parameters are listed in Table I. Using the bootstrap algorithm [15] we calculated the 95% confidence intervals for all simulated curves. These intervals are indicated by the vertical bars in the simulated curves.

A. Estimation Performance

The estimation performance is presented in Fig. 3, Fig. 4 and Fig. 5 in terms of MSE for the FFO/RFO and error probability for the IFO. In the simulated 1000 subframes transmission, FFO and IFO estimations are carried out in every fifth subframe, leading to a relatively large confidence interval compared to the RFO estimation curves.

In Fig. 3 and Fig. 4, it is shown that for AWGN transmission, the simulated curves agree quite well with the calculated theoretical MSE. For ITU Pedestrian B (PedB) [12] channels with time dispersion, the MSE of the FFO estimator saturates around 10^{-5} since the beginning of the CP is corrupted by the delayed version of the previous OFDM symbol. As long as the FFO estimation error does not exceed the estimation range of the RFO estimator, this does not affect the overall estimation performance.

For the IFO estimation, errors only occur for the SISO transmission in PedB channel (Fig. 5). The error in the IFO estimation results in a subcarrier mismatch which fails the RFO estimation where correct reference symbol extraction is required (Fig 3, SNR < 10 dB).

B. System Performance

In order to investigate the impact of the CFO on the system performance when no CFO compensation is employed, we introduced 100 logarithmically spaced CFOs between 10^{-4} and 10^{-1} subcarrier spacings and observe the variation of the physical layer coded throughput for a series of CQI values (Fig. 6 and Fig. 7). The simulated throughput curves drop sharply when the CFOs reach certain levels. The higher CQIs

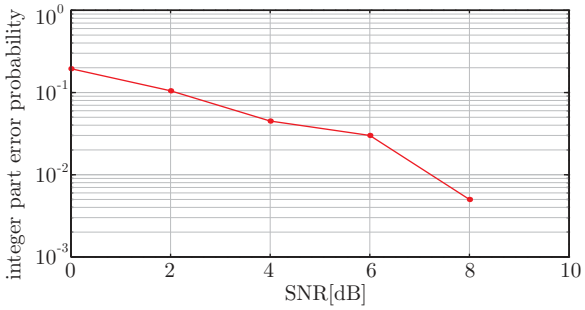

Fig. 5. Error probability of the IFO estimation.

which have larger modulation scheme and higher coding rate also require more accurate frequency synchronization.

The uncoded Bit Error Ratio (BER) curves for simulations in AWGN and PedB channels are shown in Fig. 8 and Fig. 9. When comparing to the perfect synchronization cases, both 1×1 SISO and 4×2 MIMO transmission show hardly any loss. The same trend is observed for the coded throughput curves in Fig. 10.

Note that CQI 15, which has the most demanding requirements on CFO compensation, requires the CFO to be less than about 10^{-3} (see Fig. 6) which corresponds to 10^{-6} of MSE. This requirement is fullfilled by our CFO compensation scheme at SNR 30 dB (see Fig. 3), explaining the negligible loss in the simulated BER and throughput curves.

VI. Conclusion

In this paper, a CFO compensation scheme for 3GPP LTE is presented and evaluated. Simulation results show that the presented three stage scheme is sufficient to compensate even relatively large CFOs in slow fading scenarios. Compared to perfect synchronization, the performance loss is hardly noticeable. Since the synchronization and reference signals in the standard are not dedicated for carrier frequency syn-

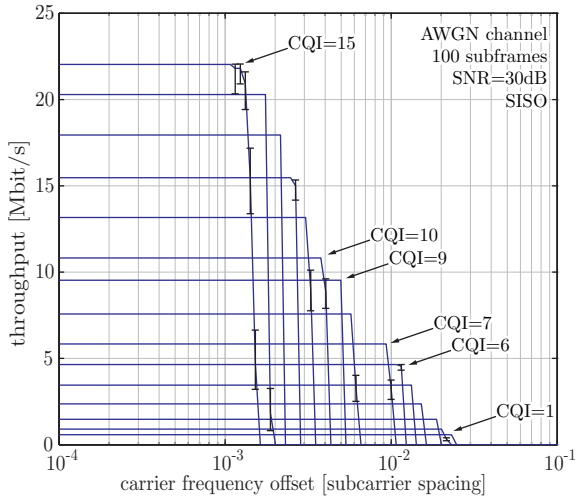

Fig. 6. Throughput of SISO transmission over an AWGN channel when CFO is introduced.

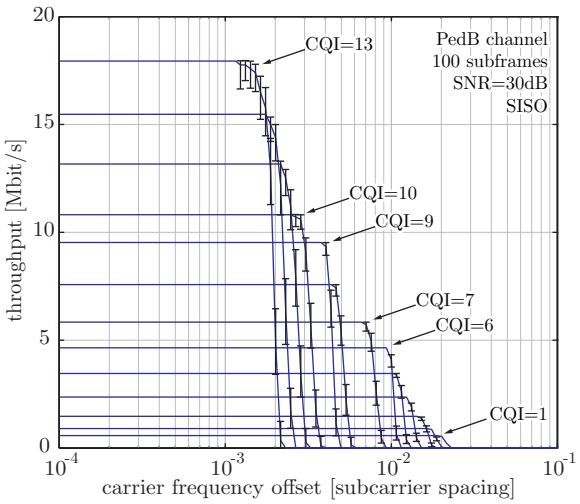

Fig. 7. Throughput of SISO transmission over a PedB channel when CFO is introduced.

chronization but mainly used for cell search and channel estimation, it is not necessary to apply more sophisticated compensation schemes to reduce the resource overhead. We plan further investigation in high mobility scenarios with fast fading channels.

ACKNOWLEDGMENTS

Funding for this research was provided by the fFORTE WIT - Women in Technology Program of the Vienna University of Technology. This program is co-financed by the Vienna University of Technology, the Ministry for Science and Research and the fFORTE Initiative of the Austrian Government. Also, this work has been co-funded by the Christian Doppler Laboratory for Wireless Technologies for Sustainable Mobility.

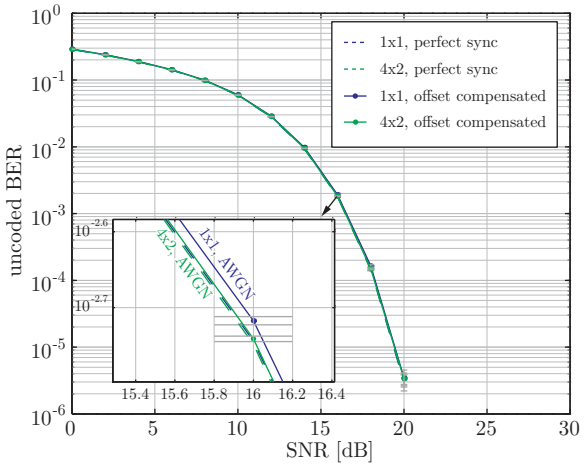

Fig. 8. Uncoded BER of CQI=9 SISO transmission in AWGN channel.

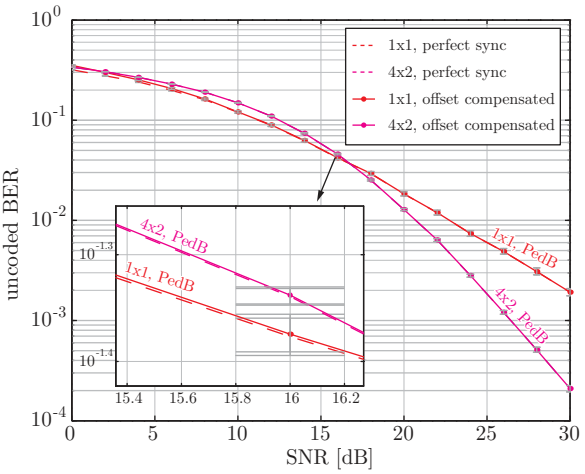

Fig. 9. Uncoded BER of CQI=9 SISO transmission in PedB channel.

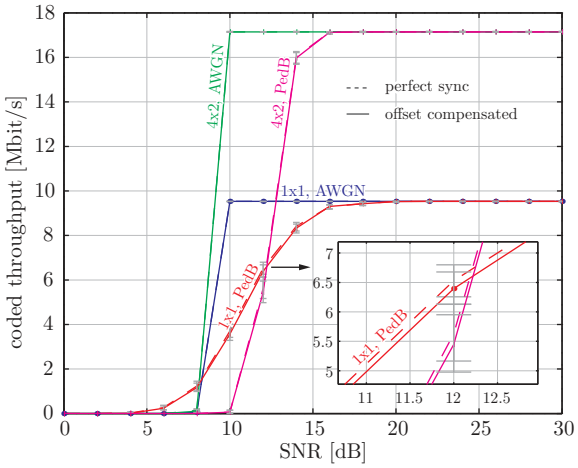

Fig. 10. Coded Throughput of CQI=9 SISO/MIMO transmission over AWGN and PedB channel.

APPENDIX I. DERIVATION OF THE THEORETICAL MSE OF THE FFO ESTIMATOR

In order to derive the theoretical MSE of the FFO estimator, we rewrite Eq. (5) as

$$\hat{\varepsilon}_{\text{FFO}} = -\frac{1}{2\pi}\arctan\frac{\Im\left\{\sum_{m=1}^{N_\text{R}}\sum_{l=1}^{N_\text{f}}\sum_{n=1}^{N_\text{g}} r_{l,n}^{(m)} r_{l,n+N}^{(m)*}\right\}}{\Re\left\{\sum_{m=1}^{N_\text{R}}\sum_{l=1}^{N_\text{f}}\sum_{n=1}^{N_\text{g}} r_{l,n}^{(m)} r_{l,n+N}^{(m)*}\right\}}, \tag{11}$$

where $\Re\{\cdot\}$ and $\Im\{\cdot\}$ are the real and imaginary operators. The estimation error can be written as

$$\begin{aligned}&\varepsilon_{\text{FFO}} - \hat{\varepsilon}_{\text{FFO}} = \\ =&\frac{1}{2\pi}\arctan\frac{\Im\left\{\sum_{m=1}^{N_\text{R}}\sum_{l=1}^{N_\text{f}}\sum_{n=1}^{N_\text{g}} r_{l,n}^{(m)} r_{l,n+N}^{(m)*} e^{j2\pi\varepsilon_{\text{FFO}}}\right\}}{\Re\left\{\sum_{m=1}^{N_\text{R}}\sum_{l=1}^{N_\text{f}}\sum_{n=1}^{N_\text{g}} r_{l,n}^{(m)} r_{l,n+N}^{(m)*} e^{j2\pi\varepsilon_{\text{FFO}}}\right\}}.\end{aligned} \tag{12}$$

When the error is small, Eq. (12) can be approximated to

$$\begin{aligned}&\varepsilon_{\text{FFO}} - \hat{\varepsilon}_{\text{FFO}} \cong \\ \cong&\frac{1}{2\pi}\frac{\Im\left\{\sum_{m=1}^{N_\text{R}}\sum_{l=1}^{N_\text{f}}\sum_{n=1}^{N_\text{g}} r_{l,n}^{(m)} r_{l,n+N}^{(m)*} e^{j2\pi\varepsilon_{\text{FFO}}}\right\}}{\Re\left\{\sum_{m=1}^{N_\text{R}}\sum_{l=1}^{N_\text{f}}\sum_{n=1}^{N_\text{g}} r_{l,n}^{(m)} r_{l,n+N}^{(m)*} e^{j2\pi\varepsilon_{\text{FFO}}}\right\}}.\end{aligned} \tag{13}$$

In order to find the real and imaginary terms, we rewrite Eq. (1) for simplicity

$$r_{l,n}^{(m)} = \left(\dot{r}_{l,n}^{(m)} + v_{l,n}^{(m)}\right) e^{j2\pi\hat{\varepsilon}_{\text{FFO}}(n+l(N+N_\text{g}))/N}, \tag{14}$$

with $\dot{r}_{l,n}^{(m)} = x_{l,n}^{(m)} * h_{l,n}^{(m)}$ denoting the received signal without CFO. Thus, we have

$$\begin{aligned}&r_{l,n}^{(m)} r_{l,n+N}^{(m)*} e^{j2\pi\varepsilon_{\text{FFO}}} = \\ =&\left(\dot{r}_{l,n}^{(m)} + v_{l,n}^{(m)}\right)\left(\dot{r}_{l,n+N}^{(m)} + v_{l,n+N}^{(m)}\right)^* e^{j2\pi(\varepsilon_{\text{FFO}}-\hat{\varepsilon}_{\text{FFO}})} \\ =&\left(\dot{r}_{l,n}^{(m)}\dot{r}_{l,n+N}^{(m)*} + \dot{r}_{l,n}^{(m)} v_{l,n+N}^{(m)*} + v_{l,n}^{(m)}\dot{r}_{l,n+N}^{(m)*} + v_{l,n}^{(m)} v_{l,n+N}^{(m)*}\right) \\ &\cdot \underbrace{e^{j2\pi(\varepsilon_{\text{FFO}}-\hat{\varepsilon}_{\text{FFO}})}}_{\approx 1 \text{ for small error}}.\end{aligned} \tag{15}$$

When relatively large SNR is assumed, there is

$$\begin{aligned}\Re\left\{\dot{r}_{l,n}^{(m)}\dot{r}_{l,n+N}^{(m)*}\right\} \gg&\Re\left\{\dot{r}_{l,n}^{(m)} v_{l,n+N}^{(m)*} + v_{l,n}^{(m)}\dot{r}_{l,n+N}^{(m)*}\right. \\ &\left. + v_{l,n}^{(m)} v_{l,n+N}^{(m)*}\right\}.\end{aligned} \tag{16}$$

Thus, the denominator in Eq. (13) becomes

$$\begin{aligned}&\Re\left\{\sum_{m=1}^{N_\text{R}}\sum_{l=1}^{N_\text{f}}\sum_{n=1}^{N_\text{g}} r_{l,n}^{(m)} r_{l,n+N}^{(m)*} e^{j2\pi\varepsilon_{\text{FFO}}}\right\} \\ =&\sum_{m=1}^{N_\text{R}}\sum_{l=1}^{N_\text{f}}\sum_{n=1}^{N_\text{g}} \dot{r}_{l,n}^{(m)}\dot{r}_{l,n+N}^{(m)*} = N_\text{R} N_\text{f} N_\text{g}\sigma_r^2,\end{aligned} \tag{17}$$

where σ_r^2 is the average signal power of the received signal in time domain.

Based on the fact that $E\{v_{l,n}^{(m)}\} = 0$, $E\{|v_{l,n}^{(m)}|^2\} = \sigma_v^2$, the variance of the nominator in Eq. (13) can be found by straightforward calculation:

$$E\{|\Im\{\cdot\}|^2\} = N_\text{R} N_\text{f} N_\text{g}\left(\sigma_v^2\sigma_r^2 + \frac{1}{2}\sigma_v^4\right) \tag{18}$$

Therefore, the MSE is given by

$$\begin{aligned}&E\{|\varepsilon_{\text{FFO}} - \hat{\varepsilon}_{\text{FFO}}|^2\} = \frac{1}{4\pi^2}\frac{E\{|\Im\{\cdot\}|^2\}}{(N_\text{R} N_\text{f} N_\text{g}\sigma_r^2)^2} = \frac{2\sigma_v^2\sigma_r^2 + \sigma_v^4}{8\pi^2 N_\text{R} N_\text{g} N_\text{f}\sigma_r^4} \\ =&\frac{2\gamma_t + 1}{8\pi^2 N_\text{R} N_\text{g} N_\text{f}\gamma_t^2} \approx \frac{1}{4\pi^2 N_\text{R} N_\text{g} N_\text{f}\gamma_t},\end{aligned} \tag{19}$$

where $\gamma_t = \sigma_r^2/\sigma_v^2 \gg 1$ is the signal-to-noise ratio of the received signal in time domain.

REFERENCES

[1] 3GPP, "Technical specification group radio access network; (E-UTRA) and (E-UTRAN); overall description; stage 2," Tech. Rep., 2008. [Online]. Available: http://www.3gpp.org/ftp/Specs/html-info/36300.htm

[2] P. H. Moose, "A technique for orthogonal frequency division multiplexing frequency offset correction," *IEEE Transactions on Communications*, vol. 42, no. 10, pp. 2908–2914, Oct 1994.

[3] J. J. van de Beek, M. Sandell, and P. O. Borjesson, "ML estimation of time and frequency offset in OFDM system," *IEEE Transactions on Signal Processing*, vol. 45, pp. 1800–1805, Jul. 1997.

[4] M. Speth, S. Fechtel, G. Fock, and H. Meyr, "Optimum receiver design for OFDM-based broadband transmission. II. a case study," *IEEE Transactions on Communications*, vol. 49, pp. 571–578, Apr 2001.

[5] D. Toumpakaris, J. Lee, and H. Lou, "Estimation of integer carrier frequency offset in OFDM systems based on the maximum likelihood principle," *IEEE Transactions on Broadcasting*, vol. 55, pp. 95–108, March 2009.

[6] Q. Wang, C. Mehlführer, and M. Rupp, "SNR optimized residual frequency offset compensation for WiMAX with throughput evaluation," in *Proc. 17th European Signal Processing Conference (EUSIPCO 2009)*, Glasgow, Scotland, Aug. 2009.

[7] Q. Wang, S. Caban, C. Mehlführer, and M. Rupp, "Measurement based throughput evaluation of residual frequency offset compensation in WiMAX," in *Proc. 51st International Symposium ELMAR-2009*, Zadar, Croatia, Sep. 2009.

[8] C. R. N. Athaudage and K. Sathananthan, "Cramer-rao lower bound on frequency offset estimation error in OFDM systems with timing error feedback compensation," in *Proc. 5th International Conference on information, Communications and Signal Processing*, Bangkok, Thailand, Dec. 2005.

[9] K. Manolakis, D. M. Gutierrez Estevez, V. Jungnickel, W. Xu, and C. Drewes, "A closed concept for synchronization and cell search in 3GPP LTE systems," in *Proc. IEEE Wireless Communication and Networking Conference (WCNC)*, Budapest, Hungary, 2009.

[10] C. Mehlführer, M. Wrulich, J. C. Ikuno, D. Bosanska, and M. Rupp, "Simulating the long term evolution physical layer," in *Proc. 17th European Signal Processing Conference (EUSIPCO 2009)*, Glasgow, Scotland, UK, Aug. 2009. [Online]. Available: http://publik.tuwien.ac.at/files/PubDat_175708.pdf

[11] 3GPP, "Technical specification group radio access network; (E-UTRA) and (E-UTRAN); physical channels and modulation; (release 8)," Tech. Rep., 2008. [Online]. Available: http://www.3gpp.org/ftp/Specs/html-info/36211.htm

[12] "Recommendation ITU-R M.1225: Guidelines for evaluation of radio transmission technologies for IMT-2000," Tech. Rep., 1997.

[13] "LTE simulator homepage." [Online]. Available: http://www.nt.tuwien.ac.at/ltesimulator/

[14] B. Stantchev and G. Fettweis, "Time-variant distortion in OFDM," *IEEE Communications Letters*, vol. 4, pp. 312–314, Oct 2000.

[15] B. Efron and D. V. Hinkley, *An Introduction to the Bootstrap (CRC Monographs on Statistics & Applied Probability 57)*, 1st ed. Chapman & Hall/CRC, 1994.